
Article:
Petrukhin, N.S., Ruderman, M.S. and Shurgalina, E.G. (2018) Phase mixing of Alfven waves in axisymmetric non-reflective magnetic plasma configurations. Monthly Notices of the Royal Astronomical Society, 474 (2). pp. 2289-2301. ISSN 0035-8711

https://doi.org/10.1093/mnras/stx2914

Monthly Notices
of the
ROYAL ASTRONOMICAL SOCIETY

MNRAS **474,** 2289–2301 (2018) doi:10.1093/mnras/stx2914
Advance Access publication 2017 November 14

Phase mixing of Alfvén waves in axisymmetric non-reflective magnetic plasma configurations

N. S. Petrukhin,[1]★ M. S. Ruderman[2,3]★ and E. G. Shurgalina[4,5]

[1]*National Research University Higher School of Economics, Moscow 101000, Russia*
[2]*School of Mathematics and Statistics, University of Sheffield, Hicks Building, Hounsfield Road, Sheffield S3 7RH, UK*
[3]*Space Research Institute (IKI), Russian Academy of Sciences, Moscow 117997, Russia*
[4]*Department of Nonlinear Geophysical Processes, Institute of Applied Physics, Nizhny Novgorod 603950, Russia*
[5]*Nizhny Novgorod State Technical University n.a. R.E. Alekseev, Nizhny Novgorod 603950, Russia*

Accepted 2017 November 6. Received 2017 October 31; in original form 2017 October 5

ABSTRACT

We study damping of phase-mixed Alfvén waves propagating in non-reflective axisymmetric magnetic plasma configurations. We derive the general equation describing the attenuation of the Alfvén wave amplitude. Then we applied the general theory to a particular case with the exponentially divergent magnetic field lines. The condition that the configuration is non-reflective determines the variation of the plasma density along the magnetic field lines. The density profiles exponentially decreasing with the height are not among non-reflective density profiles. However, we managed to find non-reflective profiles that fairly well approximate exponentially decreasing density. We calculate the variation of the total wave energy flux with the height for various values of shear viscosity. We found that to have a substantial amount of wave energy dissipated at the lower corona, one needs to increase shear viscosity by seven orders of magnitude in comparison with the value given by the classical plasma theory. An important result that we obtained is that the efficiency of the wave damping strongly depends on the density variation with the height. The stronger the density decrease, the weaker the wave damping is. On the basis of this result, we suggested a physical explanation of the phenomenon of the enhanced wave damping in equilibrium configurations with exponentially diverging magnetic field lines.

Key words: MHD – plasmas – waves – Sun: corona – Sun: oscillations.

1 INTRODUCTION

The solar coronal heating is an outstanding problem in solar physics. For a few decades, Alfvén waves remain a popular mechanism for heating the coronal plasma. Alfvén waves can efficiently transport the energy from the lower part of the solar atmosphere to the corona. It was shown in a recent paper by Soler et al. (2017) that torsional Alfvén waves with periods of the order of second are almost completely damp in the chromosphere; waves with periods of a few minutes are strongly reflected mainly from the transitional region; however, a large part of the energy of waves with the periods of the order of minute is transmitted in the corona. Another important result obtained by Soler et al. (2017) is that the magnetic tube expansion facilitates the Alfvén energy transmission in the corona. However, for typical coronal conditions, Alfvén waves can propagate through the corona practically without damping because they do not perturb the plasma density.

Heyvaerts & Priest (1983) suggested Alfvén wave phase mixing as a mechanism that can enormously enhance the Alfvén wave damping in weakly dissipative plasmas. Phase mixing causes large gradients in the direction perpendicular to the wave propagation direction to build up. As a result, the damping length is proportional to $\mathrm{Re}^{1/3}$ rather than Re as it is in a homogeneous plasma, where Re is either the viscous or resistive Reynolds number. The possibility of efficient Alfvén wave damping in weakly dissipative plasmas made phase mixing a popular mechanism for coronal heating. For a review of the recent progress in the theory of coronal heating by waves, see a review by Arregui (2015).

In spite that phase mixing strongly enhances the Alfvén wave damping, still it is not enough to cause substantial damping in the lower solar corona. This prompted researchers to search for additional mechanisms to further enhance the wave damping. Malara, Primavera & Veltri (1996) showed that Alfvén wave phase mixing can generate compressible perturbations. These perturbations are subjected to non-linear steepening that leads to the appearance of shocks. This mechanism was also studied by Nakariakov, Roberts & Murawski (1997), Botha et al. (2000), Tsiklauri, Arber &

★ E-mail: npetruhin@hse.ru (NSP); M.S.Ruderman@sheffield.ac.uk (MSR)

Nakariakov (2001, 2002), Tsiklauri & Nakariakov (2002) and Tsiklauri, Nakariakov & Rowlands (2003).

The efficiency of Alfvén wave damping due to phase mixing also strongly depends on the geometry of equilibrium. Ruderman, Nakariakov & Roberts (1998) studied the Alfvén wave phase mixing in two-dimensional magnetic plasma configurations under the assumption that the curvature of the magnetic field lines and the characteristic scale of the Alfvén speed variation along the magnetic field lines are both much larger than the wavelength. The solution was obtained using the Wentzel–Kramers–Brillouin (WKB) method. In particular, Ruderman et al. (1998) showed that strong divergence of the magnetic field lines can substantially enhance the efficiency of the Alfvén wave damping due to phase mixing. While the damping length in an equilibrium with the straight magnetic field lines and the Alfvén speed only varying in the direction orthogonal to the magnetic field direction are proportional to $\mathrm{Re}^{1/3}$, in an equilibrium with the exponentially divergent magnetic field lines they are proportional to $\ln(\mathrm{Re})$. This result was confirmed by Smith, Tsiklauri & Ruderman (2007) who studied the problem of the Alfvén wave damping due to phase mixing in an equilibrium with the exponentially divergent magnetic field lines both analytically and numerically. The interest to studying wave propagation in magnetic plasma configurations with strongly divergent magnetic field lines was boosted by the observation that in the chromosphere and lower corona the cross-section area of open magnetic tubes can increase by a few hundred times (Tsuneta et al. 2008).

If we consider Alfvén wave propagation, for example, in plumes in coronal holes, then for waves with periods of the order of one minute the wavelengths can be comparable with the characteristic scale of variation of background quantities. In that case, the WKB approximation cannot be used and, in general, the study of phase mixing is only possible numerically. However, there is one exception. Analytical study is still possible when the waves propagate in so-called non-reflective equilibria. In these equilibria, Alfvén waves propagate without reflection.

Non-reflective wave propagation was investigated in various branches of sciences. It was studied in plasma physics (Ginzburg 1970), oceanography (Brekhovskikh 1980; Didenkulova, Pelinovsky & Soomere 2008; Grimshaw, Pelinovsky & Talipova 2010), acoustics (Ibragimov & Rudenko 2004) and atmospheric science (Petrukhin, Pelinovsky & Batsyna 2011). Recently, the theory of non-reflective wave propagation has been applied to solar physics. Petrukhin, Pelinovsky & Batsyna (2012) studied non-reflective vertical propagation of acoustic waves in the solar atmosphere. Ruderman et al. (2013) and Petrukhin, Ruderman & Pelinovsky (2015) studied non-reflective propagation of kink waves along thin magnetic flux tubes.

Recently, Ruderman & Petrukhin (2017) studied Alfvén wave phase mixing in non-reflective planar magnetic plasma equilibria. In this paper, we aim to extend their analysis to axisymmetric equilibria. The paper is organized as follows. In the next section, we formulate the problem and present the governing equation describing the Alfvén wave propagation. In Section 3, we introduce curvilinear coordinates. In Section 4, we present the general theory of non-reflective Alfvén wave propagation in axisymmetric magnetic plasma equilibria. In Section 5, we consider viscous damping of phase-mixed Alfvén waves. In Section 6, we apply the general theory to the Alfvén wave damping in magnetic plasma equilibria with exponentially divergent magnetic field lines. Section 7 contains the summary of obtained results and our conclusions.

2 PROBLEM FORMULATION

We consider the Alfvén wave propagation in axisymmetric equilibria where all equilibrium quantities depend on r and z in cylindrical coordinates r, θ, z with the z-axis vertical. The θ-component of the equilibrium magnetic field is zero. The plasma beta in the solar corona is very low, which implies that the equilibrium magnetic field must be force-free. A force-free axisymmetric magnetic field without azimuthal component is always potential. Hence, the equilibrium magnetic field $\boldsymbol{B} = (B_r, 0, B_z)$ can be expressed in terms of magnetic potential ϕ. It can also be expressed in terms of the magnetic flux function ψ. As a result, we have

$$\frac{B_r}{B_0} = \frac{\partial \phi}{\partial r} = -\frac{H}{r}\frac{\partial \psi}{\partial z}, \quad \frac{B_z}{B_0} = \frac{\partial \phi}{\partial z} = \frac{H}{r}\frac{\partial \psi}{\partial r}, \tag{1}$$

where B_0 is a constant equal to the characteristic value of the magnetic field and H is the characteristic spatial scale of equilibrium quantity variation. Since ψ is defined with the accuracy up to an additive constant, we impose the condition that $\psi = 0$ at $r = 0$. Below we use ϕ and ψ as new curvilinear coordinates in the $\theta = \mathrm{const}$ plane. It follows from equation (1) that $\nabla\phi \cdot \nabla\psi = 0$. This means that the curvilinear coordinate system (ϕ, ψ) is orthogonal. The ϕ coordinate lines coincide with the magnetic field lines, while the ψ coordinate lines are orthogonal to the magnetic field lines. We consider the plasma density ρ as a free function. If this function is given, then the plasma pressure and temperature are determined by the projection of the equilibrium equation on the magnetic field direction and the ideal gas law.

Below we study Alfvén waves where only the θ-components of the velocity and magnetic field, v and b, are non-zero, while all other quantities remain unperturbed. To describe these waves, we use the θ-components of the momentum and induction equation. The only dissipative process that we take into account is shear viscosity, while we neglect resistivity. Some authors (e.g. Heyvaerts & Priest 1983) took both shear viscosity and resistivity into account. As a result, they obtained that the term describing dissipation in the equation governing the Alfvén wave propagation is multiplied by the sum of the kinematic viscosity and magnetic diffusion. In the corona, these quantities are of the same order. This implies that neglecting one of them can only reduce the efficiency of wave damping by a factor of the order of unity. On the other hand, neglecting resistivity simplifies the analysis because it enables the magnetic field perturbation to be easily eliminated from the governing equations. The linearized governing equations are

$$\rho\frac{\partial v}{\partial t} = \frac{1}{\mu_0 r}\boldsymbol{B}\cdot\nabla(rb) + \frac{1}{r}\frac{\partial}{\partial r}\left(\rho\nu r\frac{\partial v}{\partial r}\right) + \frac{\partial}{\partial z}\left(\rho\nu\frac{\partial v}{\partial z}\right), \tag{2}$$

$$\frac{\partial b}{\partial t} = r\boldsymbol{B}\cdot\nabla\left(\frac{v}{r}\right), \tag{3}$$

where μ_0 is the magnetic permeability of free space and ν the kinematic viscosity. We now introduce the angular velocity $u = v/r$. The last two terms on the right-hand side of equation (2) can be transformed to

$$\frac{1}{r}\frac{\partial(\rho\nu r^2)}{\partial r}\frac{\partial u}{\partial r} + \frac{1}{r}\frac{\partial(\rho\nu r u)}{\partial r} + r\frac{\partial(\rho\nu)}{\partial z}\frac{\partial u}{\partial z} + \rho\nu r\left(\frac{\partial^2 u}{\partial r^2} + \frac{\partial^2 u}{\partial z^2}\right). \tag{4}$$

Below we consider the Alfvén wave propagation in weakly dissipative plasmas. The viscosity is only important when there are large gradients. We will see that, because of phase mixing, such gradients of perturbed quantities are formed. We denote the spatial scale of the velocity variation when these large gradients are developed as

$l_{\rm dis}$. On the other hand, the gradients of equilibrium quantities do not change and the spatial scale of their variation remains equal to $l_{\rm eq} \gg l_{\rm dis}$. As a result, the first three terms in equation (4) are of the order of $\rho\nu r u/l_{\rm eq} l_{\rm dis}$, while the fourth term is of the order of $\rho\nu r u/l_{\rm dis}^2$. We see that the ratio of the first three terms in equation (4) to the last term is of the order of $l_{\rm dis}/l_{\rm eq} \ll 1$. This estimate enables to neglect the first three terms in comparison with the last one and use the approximation

$$\frac{1}{r}\frac{\partial}{\partial r}\left(\rho\nu r\frac{\partial v}{\partial r}\right)+\frac{\partial}{\partial z}\left(\rho\nu\frac{\partial v}{\partial z}\right)\approx\rho\nu r\left(\frac{\partial^2 u}{\partial r^2}+\frac{\partial^2 u}{\partial z^2}\right). \tag{5}$$

Then, using equation (2) to eliminating b, we obtain the equation for u,

$$\rho\frac{\partial^2 u}{\partial t^2}=\frac{\boldsymbol{B}\cdot\nabla(r^2\boldsymbol{B}\cdot\nabla u)}{\mu_0 r^2}+\rho\nu\left(\frac{\partial^3 u}{\partial t\partial r^2}+\frac{\partial^3 u}{\partial t\partial z^2}\right). \tag{6}$$

This equation is used below to study the Alfvén wave damping due to phase mixing.

3 INTRODUCING CURVILINEAR COORDINATES

We now make the variable substitution and use ϕ and ψ as the independent variables. Then we have the following expressions for the partial derivatives with respect to r and z:

$$\frac{\partial}{\partial r}=\frac{B_r}{B_0}\frac{\partial}{\partial\phi}+\frac{rB_z}{HB_0}\frac{\partial}{\partial\psi},\quad \frac{\partial}{\partial z}=\frac{B_z}{B_0}\frac{\partial}{\partial\phi}-\frac{rB_r}{HB_0}\frac{\partial}{\partial\psi}. \tag{7}$$

It follows from this equation that

$$\boldsymbol{B}\cdot\nabla f=\frac{B^2}{B_0}\frac{\partial f}{\partial\phi}, \tag{8}$$

where f is any function. Below we will see that the large gradients only appear in the ψ-direction, which is the direction perpendicular to the magnetic field lines. The derivative with respect to ψ is inversely proportional to $l_{\rm dis}$, while the derivative with respect to ϕ is inversely proportional to the wavelength. Under a viable assumption that the wavelength is much larger than $l_{\rm dis}$, the second derivative with respect to ψ strongly dominates all other derivatives and we can use the approximate expression

$$\frac{\partial^2 u}{\partial r^2}+\frac{\partial^2 u}{\partial z^2}\approx\frac{r^2B^2}{H^2B_0^2}\frac{\partial^2 u}{\partial\psi^2}. \tag{9}$$

Using this approximation and equations (7) and (8), we transform equation (6) to

$$\frac{\partial^2 u}{\partial t^2}-\frac{V_{\rm A}^2}{r^2}\frac{\partial}{\partial\phi}\left(\frac{r^2B^2}{B_0^2}\frac{\partial u}{\partial\phi}\right)=\frac{\nu r^2B^2}{H^2B_0^2}\frac{\partial^3 u}{\partial t\partial\psi^2}, \tag{10}$$

where

$$V_{\rm A}^2=\frac{B^2}{\mu_0\rho} \tag{11}$$

is the Alfvén speed.

4 NON-REFLECTIVE PROPAGATION OF ALFVÉN WAVES

In this section, we describe how equation (10) can be reduced to an equation with constant coefficients when $\nu = 0$. The reduction of the wave equation with the variable phase speed to the Klein–Gordon equation with constant coefficients is described in many papers (see e.g. Ruderman et al. 2013).

We search for the solution to equation (10) in the form

$$u(t,\phi,\psi)=A(\phi,\psi)\Phi(t,h(\phi,\psi),\psi), \tag{12}$$

where $A(\phi,\psi)$, $h(\phi,\psi)$ and $\Phi(t,h(\phi,\psi),\psi)$ are the functions to be determined. Substituting this expression in equation (10), we obtain

$$\begin{aligned}&\frac{\partial^2\Phi}{\partial t^2}-V_{\rm A}^2\frac{B^2}{B_0^2}\left(\frac{\partial h}{\partial\phi}\right)^2\frac{\partial^2\Phi}{\partial h^2}\\&\quad-V_{\rm A}^2\left[\frac{r^2B^2}{AB_0^2}\frac{\partial A}{\partial\phi}\frac{\partial h}{\partial\phi}+\frac{1}{A}\frac{\partial}{\partial\phi}\left(\frac{r^2AB^2}{B_0^2}\frac{\partial h}{\partial\phi}\right)\right]\frac{\partial\Phi}{\partial h}\\&\quad-\frac{V_{\rm A}^2\Phi}{r^2A}\left[\frac{\partial}{\partial\phi}\left(\frac{r^2B^2}{B_0^2}\frac{\partial A}{\partial\phi}\right)\right]=\frac{\nu r^2B^2}{H^2B_0^2}\frac{\partial\Xi}{\partial t},\end{aligned} \tag{13}$$

where

$$\begin{aligned}\Xi=&\frac{1}{A}\frac{\partial^2(A\Phi)}{\partial\psi^2}+\frac{2}{A}\frac{\partial h}{\partial\psi}\frac{\partial}{\partial\psi}\left(A\frac{\partial\Phi}{\partial h}\right)\\&+\frac{\partial^2 h}{\partial\psi^2}\frac{\partial\Phi}{\partial h}+\left(\frac{\partial h}{\partial\psi}\right)^2\frac{\partial^2\Phi}{\partial h^2}.\end{aligned} \tag{14}$$

Now we impose the condition that the coefficient at the second derivative of Φ with respect to h on the left-hand side of this equation is equal to V_0^2, and the coefficient at the first derivative is zero, where $V_0 = B_0(\mu_0\rho_0)^{-1/2}$ is the characteristic value of the Alfvén speed and ρ_0 is the density at the coordinate origin ($r = z = 0$):

$$\frac{B^2V_{\rm A}^2}{B_0^2V_0^2}\left(\frac{\partial h}{\partial\phi}\right)^2=1, \tag{15}$$

$$r^2B^2\frac{\partial A}{\partial\phi}\frac{\partial h}{\partial\phi}+\frac{\partial}{\partial\phi}\left(r^2AB^2\frac{\partial h}{\partial\phi}\right)=0. \tag{16}$$

Below we consider waves propagating in the positive ϕ-direction. Then it follows from equation (15) that

$$h=B_0V_0\int_{\phi_1}^{\phi}\frac{{\rm d}\phi'}{BV_{\rm A}}, \tag{17}$$

where ϕ_1 is a function of ψ that, at present, we do not specify. Using equation (17) to integrate equation (16), we obtain

$$A=A_0(\psi)(H/r)(\rho_0/\rho)^{1/4}, \tag{18}$$

where $A_0(\psi)$ is an arbitrary function satisfying the condition that there is a non-zero limit of $A_0(\psi)r^{-1}$ as $\psi\to 0$. Now equation (13) reduces to

$$\frac{\partial^2\Phi}{\partial t^2}-V_0^2\frac{\partial^2\Phi}{\partial h^2}=\frac{V_{\rm A}^2\Phi}{r^2A}\frac{\partial}{\partial\phi}\left(\frac{r^2B^2}{B_0^2}\frac{\partial A}{\partial\phi}\right)+\frac{\nu r^2B^2}{H^2B_0^2}\frac{\partial\Xi}{\partial t}. \tag{19}$$

If we take $\nu = 0$, then this equation reduces to the Klein–Gordon equation. In general, this Klein–Gordon equation has one variable coefficient. This causes reflection of a wave driven at a surface $\phi = \phi_1(\psi)$ and propagating in the positive ϕ-direction. It only can propagate without reflection if the coefficient at Φ in equation (19) is constant. However, we must keep in mind that ψ is present in equation (19) as a parameter, so this constant can depend on ψ. Hence, we impose the condition that the coefficient at Φ in equation (19) only depends on ψ,

$$\frac{V_{\rm A}^2}{r^2A}\frac{\partial}{\partial\phi}\left(\frac{r^2B^2}{B_0^2}\frac{\partial A}{\partial\phi}\right)=\sigma(\psi), \tag{20}$$

where $\sigma(\psi)$ is an arbitrary function.

When $\nu = 0$ and A satisfies equation (20), equation (19) is a Klein–Gordon equation with constant coefficients (where ψ is present as a parameter). It admits a solution $\Phi = \Phi_0 \exp(\mathrm{i}kh - \mathrm{i}\omega t)$, where Φ_0 is a constant, and k and ω are related by

$$\omega^2 + \sigma(\psi) = V_0^2 k^2. \tag{21}$$

We see that waves with arbitrary frequency can propagate along a particular magnetic field line when $\sigma > 0$, while only waves with $\omega > \omega_{\rm cut}$ can propagate when $\sigma < 0$, where the cutoff frequency $\omega_{\rm cut}$ is defined by

$$\omega_{\rm cut}^2 = -\sigma(\psi). \tag{22}$$

Finally, when $\sigma = 0$, we obtain $\omega^2 = V_0^2 k^2$ and, again, waves with arbitrary frequencies can propagate.

5 ALFVÉN WAVE DAMPING DUE TO PHASE MIXING

We now study the damping of Alfvén waves due to phase mixing. In this section, we closely follow Ruderman & Petrukhin (2017). Hence, we only briefly outline the analysis omitting the details. We impose the boundary condition

$$u = u_0(t, \psi) \quad \text{at } \phi = \phi_1(\psi). \tag{23}$$

Then we take u and Φ proportional to $\exp(-\mathrm{i}\omega t)$. As a result, equation (19) is transformed to

$$V_0^2 \frac{\partial^2 \Phi}{\partial h^2} + \lambda^2 \Phi = \frac{\mathrm{i}\omega \nu r^2 B^2 \Xi}{H^2 B_0^2}, \tag{24}$$

where

$$\lambda^2 = \omega^2 + \sigma(\psi). \tag{25}$$

Below we assume that $\lambda^2 > 0$. Using equations (12), (17) and (18), we obtain from equation (23)

$$\Phi = A_0^{-1}(\psi) r^{1/2} \rho^{1/4} u_0(t, \psi) \equiv \Phi_0(t, \psi) \quad \text{at } h = 0. \tag{26}$$

We also assume that the characteristic distance of damping due to phase mixing is much greater than the characteristic distance of variation of Φ with respect to h. In accordance with this assumption, we introduce the 'slow' variable $h_1 = \epsilon h$, where $\epsilon \ll 1$.

To characterize the viscosity magnitude, we introduce the Reynolds number $\mathrm{Re} = HV_0/\nu$ (we recall that H is the characteristic spatial scale of variation of equilibrium quantities). We assume that the characteristic wavelength is also H. Below we also assume that the viscosity is weak, $\mathrm{Re} \gg 1$, and introduce the scaled kinematic viscosity $\bar{\nu} = \mathrm{Re}\,\nu$. The relation between ϵ and Re will be defined later. Then equation (24) is rewritten as

$$\epsilon^2 \frac{\partial^2 \Phi}{\partial h_1^2} + \frac{\lambda^2}{V_0^2} \Phi = \frac{\mathrm{i}\omega \bar{\nu} r^2 B^2 \widetilde{\Xi}}{H^2 V_0^2 B_0^2 \,\mathrm{Re}}, \tag{27}$$

where $\widetilde{\Xi}$ is given by equation (14) with h_1 substituted for h. Now we use the standard WKB method and look for the solution to this equation in the form

$$\Phi = Q(h_1, \psi) \exp[\mathrm{i}\epsilon^{-1} \Theta(h_1, \psi)] \tag{28}$$

(see e.g. Bender & Orszag 1999). Substituting this expression in equation (27) and using the expression for $\widetilde{\Xi}$, we obtain

$$\epsilon^2 \frac{\partial^2 Q}{\partial h_1^2} + 2\mathrm{i}\epsilon \frac{\partial Q}{\partial h_1} \frac{\partial \Theta}{\partial h_1} + \mathrm{i}\epsilon Q \frac{\partial^2 \Theta}{\partial h_1^2} - Q \left(\frac{\partial \Theta}{\partial h_1} \right)^2 + \frac{\lambda^2}{V_0^2} Q = -\frac{\mathrm{i}\epsilon^{-2} \omega \bar{\nu} r^2 B^2 Q}{H^2 V_0^2 B_0^2 \mathrm{Re}} \left[\left(\frac{\partial h_1}{\partial \psi} \right)^2 \left(\frac{\partial \Theta}{\partial h_1} \right)^2 + \mathcal{O}(\epsilon) \right]. \tag{29}$$

First, we assume that the right-hand side is much smaller than the two largest terms on the left-hand side of this equation, which are the last and next-to-last terms. Then we collect the terms of the order of unity in equation (29) to obtain

$$\left(\frac{\partial \Theta}{\partial h_1} \right)^2 = \frac{\lambda^2}{V_0^2}. \tag{30}$$

This approximation is usually called the approximation of geometrical optics (e.g. Bender & Orszag 1999). It determines the shape of rays along which the waves propagate. Only considering waves propagating in the positive ϕ-direction, we obtain from equation (30)

$$\Theta = \frac{h_1 \lambda(\psi)}{V_0}, \tag{31}$$

where we arbitrarily take $\Theta = 0$ at $h_1 = 0$. In the next-order approximation, we collect terms of the order of ϵ. This approximation is usually called the approximation of physical optics. It determines the spatial evolution of the wave amplitude. The right-hand side of equation (29) describes the viscous wave damping due to phase mixing. Hence, we define the relation between Re and ϵ in such a way that the right-hand side of equation (29) contributes in the approximation of physical optics. In accordance with this, we take $\mathrm{Re} = \epsilon^{-3}$. Then we obtain

$$2 \frac{\partial Q}{\partial h_1} \frac{\partial \Theta}{\partial h_1} + Q \frac{\partial^2 \Theta}{\partial h_1^2} = -\frac{\omega \bar{\nu} r^2 B^2 Q}{H^2 V_0^2 B_0^2 \,\mathrm{Re}} \left(\frac{\partial h_1}{\partial \psi} \right)^2 \left(\frac{\partial \Theta}{\partial h_1} \right)^2. \tag{32}$$

Using equation (31) and returning to the original variables, we transform equation (32) to

$$\frac{\partial Q}{\partial h} = -\frac{\omega \nu \lambda r^2 B^2}{2H^2 B_0^2 V_0^3} \left(\frac{\partial h}{\partial \psi} \right)^2. \tag{33}$$

With the aid of equation (17), we transform this equation to

$$\frac{\partial Q}{\partial \phi} = -\Upsilon(\phi, \psi) Q, \quad \Upsilon(\phi, \psi) = \frac{\omega \nu \lambda r^2 B}{2H^2 B_0 V_0^2 V_{\rm A}} \left(\frac{\partial h}{\partial \psi} \right)^2. \tag{34}$$

Obviously, we can assume that Q is real. Equation (34) determines the spatial evolution of the Alfvén wave amplitude. We will also use the expressions for the velocity and magnetic field perturbation. Using equations (12), (18) and (28), we obtain in the leading-order approximation with respect to ϵ

$$u = Q A_0(\psi) \frac{H}{r} \left(\frac{\rho_0}{\rho} \right)^{1/4} \exp[\mathrm{i}(h\lambda/V_0 - \omega t)]. \tag{35}$$

To obtain the expression for b, we use equation (3). It is straightforward to see that the expression for b contains two terms. The first term comes from differentiating Q, and it is proportional to ν. The second term comes from differentiating the exponent in equation (35), and it does not contain ν. It is easy to show that the ratio of the first term to the second one is of the order of ϵ. Hence, in the leading-order approximation with respect to ϵ, we obtain

$$b = -\mu_0^{1/2} H Q A_0(\psi) \frac{\lambda}{\omega} (\rho\rho_0)^{1/4} \exp[\mathrm{i}(h\lambda/V_0 - \omega t)]. \tag{36}$$

6 ALFVÉN WAVE PHASE MIXING IN EQUILIBRIA WITH EXPONENTIALLY DIVERGENT MAGNETIC FIELD LINES

6.1 Equilibrium state

Ruderman & Petrukhin (2017) studied the Alfvén wave damping due to phase mixing in various planar equilibria. The most interesting result that they obtained is that this damping is much more efficient in an equilibrium with exponentially divergent magnetic field lines than that in an equilibrium with straight magnetic field lines. In this paper, we only consider an equilibrium with exponentially divergent magnetic field lines. Substituting $\boldsymbol{B} = \nabla\phi$ in the equation $\nabla \cdot \boldsymbol{B} = 0$, we obtain $\nabla^2\phi = 0$. We search for the solution to this equation in the form $\phi = \mathrm{e}^{-z/H}F(r)$. Then we obtain

$$\frac{1}{r}\frac{\mathrm{d}}{\mathrm{d}r}\left(r\frac{\mathrm{d}F}{\mathrm{d}r}\right) + \frac{F}{H^2} = 0. \tag{37}$$

The solution to this equation is $F(r) = -HJ_0(r/H)$, where J_0 is the Bessel function of the first kind and zero order, and we arbitrarily choose the proportionality coefficient equal to $-H$. Hence, ϕ is given by

$$\phi = -H\mathrm{e}^{-z/H}J_0(r/H). \tag{38}$$

Now, using equation (1), the relation $J_0'(z) = -J_1(z)$ (Abramowitz & Stegun 1964) and taking into account that ψ/r must be regular at $r = 0$, we obtain

$$\psi = r\mathrm{e}^{-z/H}J_1(r/H), \tag{39}$$

where J_1 is the Bessel function of the first kind and first order. Using equation (1), we obtain

$$B_r = B_0\mathrm{e}^{-z/H}J_1(r/H), \quad B_z = B_0\mathrm{e}^{-z/H}J_0(r/H). \tag{40}$$

It follows from equations (38)–(40) that

$$B^2 = B_0^2\left(\frac{\phi^2}{H^2} + \frac{\psi^2}{r^2}\right). \tag{41}$$

We see that, in contrast to the planar case, we cannot explicitly express B^2 in terms of ϕ and ψ. The dependence of r on the curvilinear coordinates is determined by the equation

$$\frac{rJ_1(r/H)}{HJ_0(r/H)} = -\frac{\psi}{\phi}. \tag{42}$$

The magnetic field lines in a plane θ = const are defined by the equation ψ = const. Using equation (39) and the approximate relation $J_1(x) \approx x/2$ valid for $x \ll 1$ (Abramowitz & Stegun 1964), we obtain that, for $r \ll H$, the equation of a magnetic field line is $r = \sqrt{2H\psi}\,\mathrm{e}^{z/2H}$. We see that the distance between two neighbouring magnetic field lines increases exponentially with z. The sketch of the equilibrium is shown in Fig. 1.

We consider the wave propagation in a magnetic tube that is narrow at its base. It is bounded by the magnetic surface determined by $\psi = \psi_\mathrm{b}$, $\psi_\mathrm{b} \ll H$. The equation of this magnetic surface is

$$z = H\ln\left(\frac{r}{\psi_\mathrm{b}}J_1(r/H)\right). \tag{43}$$

Then the dependence of the magnetic tube radius R on the height z is given by the solution to this equation considered as an equation for r. The tube radius R_0 at the base ($z = 0$) is determined by the equation

$$\psi_\mathrm{b} = R_0J_1(R_0/H). \tag{44}$$

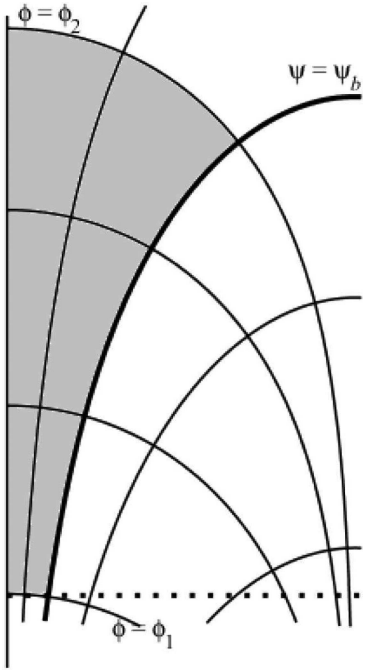

Figure 1. Equilibrium with divergent magnetic field lines. The curvilinear coordinates are shown in the plane θ = const. The vertical curves are the magnetic field lines defined by the equation ψ = const. The horizontal curves are defined by the equation ϕ = const. The thick vertical curve is the boundary of the region where the wave propagation is considered. It is defined by the equation $\psi = \psi_\mathrm{b}$. The thick horizontal line is defined by the equation $\phi = \phi_1$. It is assumed that the wave is driven at this line. The dotted line shows the level $z = 0$.

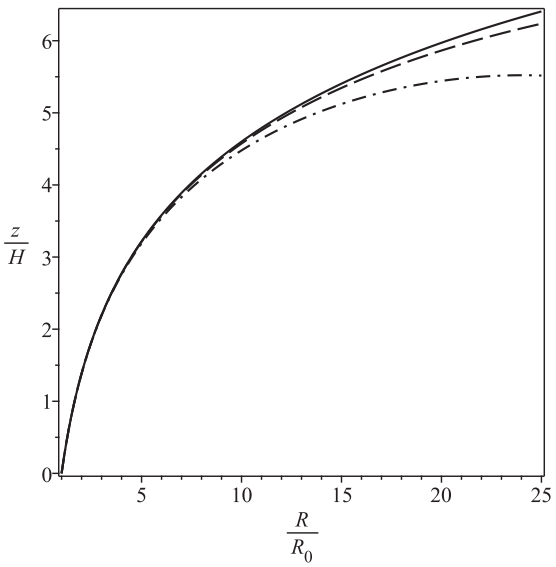

Figure 2. Dependence on the magnetic tube radius on z. The solid, dashed and dash–dotted lines correspond to the tube radius at its base equal to $0.02H$, $0.05H$ and $0.1H$, respectively.

Then we can rewrite equation (43) as

$$RJ_1(R/H) = \mathrm{e}^{z/H}R_0J_1(R_0/H). \tag{45}$$

The dependence of R on z for various values of the tube radius at its base, R_0, is shown in Fig. 2.

Using the relation (Abramowitz & Stegun 1964)

$$x J_1'(x) + J_1 = x J_0(x), \tag{46}$$

we obtain that the boundary magnetic field line reaches its maximum height at $r = Hj_1$, where j_1 is the first zero of $J_0(x)$. This maximum height is given by

$$z_\mathrm{m} = H \ln\left(\frac{Hj_1}{\psi_\mathrm{b}} J_1(j_1)\right). \tag{47}$$

It follows from equation (38) that $\phi = 0$ at $r = Hj_1$. When r increases beyond Hj_1, the boundary field line goes down. Below we consider the wave propagation in a domain bounded from below by the line $\phi = \phi_1$. We now define ϕ_1 by the condition that it intersects the magnetic tube axis at $z = 0$. It follows from this condition that $\phi_1 = -H$. Using the condition that the tube radius at the base is much smaller than H, we obtain from equations (38) and (39) that the line $\phi = \phi_1$ intersects the tube boundary at the point with the coordinates

$$r \approx \sqrt{2H\psi_\mathrm{b}}, \quad z \approx -\frac{\psi_\mathrm{b}}{2}. \tag{48}$$

We also restrict the domain where we study the wave propagation by the line $\phi = \phi_2 = \text{const}$ that intersects the boundary field line below $z = z_\mathrm{m}$. Hence, finally this domain is defined by the inequalities $\phi_1 \le \phi \le \phi_2 < 0$ and $0 \le \psi \le \psi_\mathrm{b}$. It is shaded in Fig. 1. Then the maximum radius of this domain is R_m defined by the equation

$$\frac{R_\mathrm{m} J_1(R_\mathrm{m}/H)}{H J_0(R_\mathrm{m}/H)} = -\frac{\psi_\mathrm{b}}{\phi_2}. \tag{49}$$

We emphasize that we do not assume that $R_\mathrm{m} \ll H$.

The function $r(\phi, \psi)$ monotonically increases from $r_\mathrm{m}(\psi)$ to $r_\mathrm{M}(\psi)$ when ϕ increases from ϕ_1 to ϕ_2, while ψ is fixed. In accordance with equation (42), the functions $r_\mathrm{m}(\psi)$ and $r_\mathrm{M}(\psi)$ are defined by

$$\frac{r_\mathrm{m} J_1(r_\mathrm{m}/H)}{J_0(r_\mathrm{m}/H)} = \psi, \quad \frac{r_\mathrm{M} J_1(r_\mathrm{M}/H)}{H J_0(r_\mathrm{M}/H)} = -\frac{\psi}{\phi_2}, \tag{50}$$

where we put $\phi_1 \approx -H$. Taking into account that $r_\mathrm{m}(\psi) \ll H$, we obtain $r_\mathrm{m}(\psi) \approx \sqrt{2H\psi}$.

We now obtain ρ as an explicit function of r and ψ. Using equation (18), we transform equation (20) to

$$r^2 B^2 \frac{\partial}{\partial \phi}\left(r^2 B^2 \frac{\partial G}{\partial \phi}\right) = \frac{B_0^4 H^4 \sigma(\psi)}{V_0^2 G^3}, \tag{51}$$

where $G = A/A_0$. We multiply both sides of this equation by $\partial G/\partial\phi$ and integrate the obtained equation. This results in

$$r^2 B^2 G \frac{\partial G}{\partial \phi} = \pm \frac{B_0^2 H^2}{V_0} \sqrt{G^2 \tau(\psi) - \sigma(\psi)}, \tag{52}$$

where $\tau(\psi)$ is an arbitrary function. Since the derivative on the left-hand side of this equation is calculated at constant ψ, it defines the dependence of G on ϕ on a particular magnetic field fine. We now use the variable r instead of ϕ and rewrite equation (52) as

$$r^2 B^2 G \frac{\partial G}{\partial r} = \pm \frac{B_0^2 H^2}{V_0} \frac{\partial \phi}{\partial r} \sqrt{G^2 \tau(\psi) - \sigma(\psi)}, \tag{53}$$

where both partial derivatives in this equation are calculated at $\psi = \text{const}$. It follows from equations (38) and (39) that

$$\phi = -\frac{H\psi J_0(r/H)}{r J_1(r/H)}. \tag{54}$$

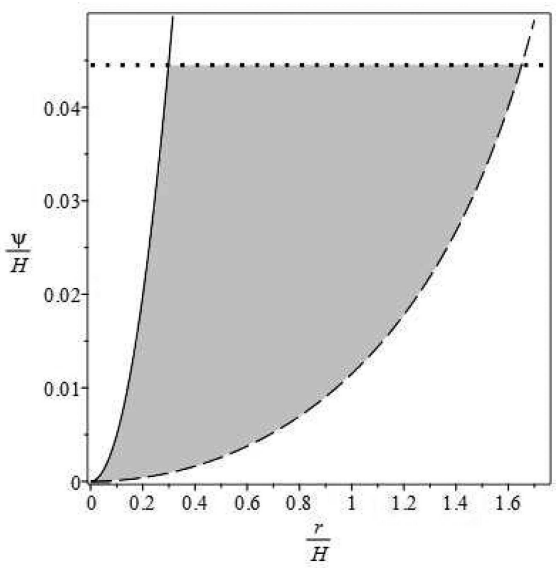

Figure 3. Area (shaded) in $r\psi$ plane defined by the inequalities (58). The upper boundary shown by the dotted line is defined by the equation $\psi = \psi_\mathrm{b}$. The solid and dashed curves are defined by the condition that ψ is equal to the right and left boundary in the second inequality in equation (58), respectively.

With the aid of this result, equation (46) and the relation $J_0'(x) = -J_1(x)$, we obtain

$$\frac{\partial \phi}{\partial r} = \frac{\psi\left[J_0^2(r/H) + J_1^2(r/H)\right]}{r J_1^2(r/H)}. \tag{55}$$

Using equations (38), (39) and (41) yields

$$r^2 B^2 = \psi^2 B_0^2 \frac{J_0^2(r/H) + J_1^2(r/H)}{J_1^2(r/H)}. \tag{56}$$

Substituting equations (55) and (56) in equation (53), we transform it to

$$G \frac{\partial G}{\partial r} = \pm \frac{H^2}{r\psi V_0} \sqrt{G^2 \tau(\psi) - \sigma(\psi)}. \tag{57}$$

This equation enables us to determine G as a function of r and ψ. After that, using equations (17) and (18), we can also determine ρ and h as functions of r and ψ. This observation inspires us to use r and ψ as independent variables in what follows. Since ψ is defined as a function of r and z by equation (39), the expressions that we will obtain will also define G, ρ and h as functions of r and z. The area in the $r\psi$ plane where we consider the wave propagation is determined by the inequalities

$$\psi \le \psi_\mathrm{b}, \quad -\frac{r\phi_2 J_1(r/H)}{H J_0(r/H)} \le \psi \le \frac{r J_1(r/H)}{J_0(r/H)}. \tag{58}$$

This area is shown in Fig. 3.

Using equations (18), (55) and (56), we transform equation (17) to

$$h = \frac{H^2}{\psi} \int_{r_\mathrm{m}}^{r} \frac{\mathrm{d}r'}{r' G^2}, \tag{59}$$

where the integral is calculated at $\psi = \text{const}$.

Now we consider four particular cases.

(i) $\tau(\psi)=\sigma(\psi)=0$. In this case, we obtain from equations (18), (57) and (59)

$$G=1/C_1(\psi),\ \ \rho=\rho_0 C_1^4(\psi)(H/r)^4,\ \ h=\frac{H^2}{\psi}C_1^2(\psi)\ln\frac{r}{r_{\rm m}(\psi)}, \tag{60}$$

where $C_1(\psi)$ is an arbitrary function. When $z\to 0$ and $r\ll H$, it follows from equation (39) that $r\approx\sqrt{2H\psi}$. Then the condition $\rho\to\rho_0$ as $z\to 0$ and $r\to 0$ implies that

$$C_1(\psi)\sqrt{\frac{H}{2\psi}}\to 1 \quad \text{as} \quad \psi\to 0. \tag{61}$$

(ii) $\tau(\psi)=0$, $\sigma(\psi)\neq 0$. Then

$$\begin{aligned} G^2&=\pm\frac{2H^2}{\psi V_0}\sqrt{-\sigma(\psi)}\ln\frac{r}{C_2(\psi)},\\ \rho&=-\frac{\rho_0\psi^2V_0^2}{4r^4\sigma(\psi)}\left(\ln\frac{r}{C_2(\psi)}\right)^{-2},\\ h&=\pm\frac{V_0}{2\sqrt{-\sigma(\psi)}}\ln\left|\frac{\ln[r/C_2(\psi)]}{\ln[r_{\rm m}(\psi)/C_2(\psi)]}\right|, \end{aligned} \tag{62}$$

where $C_2(\psi)$ is an arbitrary positive function. Obviously, these expressions are only valid when $\sigma(\psi)<0$. The condition $\rho\to\rho_0$ as $z\to 0$ and $r\to 0$ implies that

$$\sigma(\psi)\left(\ln\frac{2H\psi}{C_2^2(\psi)}\right)^2\to 1 \quad \text{as} \quad \psi\to 0. \tag{63}$$

(iii) $\sigma(\psi)=0$ and $\tau(\psi)\neq 0$. It follows from equations (18) and (57) that

$$\begin{aligned} G&=\pm\frac{H^2\sqrt{\tau(\psi)}}{\psi V_0}\ln\frac{r}{C_3(\psi)},\\ \rho&=\frac{\rho_0\psi^4V_0^4}{r^4H^4\tau^2(\psi)}\left(\ln\frac{r}{C_3(\psi)}\right)^{-4},\\ h&=\frac{\psi V_0^2}{H^2\tau(\psi)}\left[\left(\ln\frac{r_{\rm m}(\psi)}{C_3(\psi)}\right)^{-1}-\left(\ln\frac{r}{C_3(\psi)}\right)^{-1}\right], \end{aligned} \tag{64}$$

where $C_3(\psi)$ is an arbitrary positive function. These expressions are only valid when $\tau(\psi)>0$. The condition $\rho\to\rho_0$ as $z\to 0$ and $r\to 0$ implies that

$$\frac{\tau(\psi)}{\psi}\left(\ln\frac{2H\psi}{C_3^2(\psi)}\right)^2\to\frac{2V_0^2}{H^3} \quad \text{as} \quad \psi\to 0. \tag{65}$$

(iv) $\sigma(\psi)\neq 0$ and $\tau(\psi)\neq 0$. This is the most general case. Using equations (18) and (57), we obtain

$$\begin{aligned} G^2&=\frac{\sigma(\psi)}{\tau(\psi)}+\frac{H^4\tau(\psi)}{\psi^2V_0^2}\left(\ln\frac{r}{C_4(\psi)}\right)^2,\\ \rho&=\frac{\rho_0H^4}{r^4}\left[\frac{\sigma(\psi)}{\tau(\psi)}+\frac{H^4\tau(\psi)}{\psi^2V_0^2}\left(\ln\frac{r}{C_4(\psi)}\right)^2\right]^{-2}, \end{aligned} \tag{66}$$

where $C_4(\psi)$ is an arbitrary positive function. The expression for h depends on the signs of $\sigma(\psi)$ and $\tau(\psi)$. The condition $\rho\to\rho_0$ as $z\to 0$ and $r\to 0$ implies that

$$\psi\left[\frac{\sigma(\psi)}{\tau(\psi)}+\frac{H^4\tau(\psi)}{4\psi^2V_0^2}\left(\ln\frac{2H\psi}{C_4^2(\psi)}\right)^2\right]\to\frac{H}{2} \quad \text{as} \quad \psi\to 0. \tag{67}$$

When $\sigma(\psi)>0$ and $\tau(\psi)>0$, we obtain

$$\begin{aligned} h=\frac{V_0}{\sqrt{\sigma(\psi)}}\Bigg[&\arctan\left(\frac{H^2\tau(\psi)}{\psi V_0\sqrt{\sigma(\psi)}}\ln\frac{r}{C_4(\psi)}\right),\\ &-\arctan\left(\frac{H^2\tau(\psi)}{\psi V_0\sqrt{\sigma(\psi)}}\ln\frac{r_{\rm m}(\psi)}{C_4(\psi)}\right)\Bigg]. \end{aligned} \tag{68}$$

When $\sigma(\psi)<0$, the expression for h is

$$\begin{aligned} h=\frac{V_0}{2\sqrt{|\sigma(\psi)|}}\ln&\left|\frac{\psi V_0\sqrt{|\sigma(\psi)|}-H^2\tau(\psi)\ln[r/C_4(\psi)]}{\psi V_0\sqrt{|\sigma(\psi)|}+H^2\tau(\psi)\ln[r/C_4(\psi)]}\right.\\ &\left.\times\frac{\psi V_0\sqrt{|\sigma(\psi)|}+H^2\tau(\psi)\ln[r_{\rm m}(\psi)/C_4(\psi)]}{\psi V_0\sqrt{|\sigma(\psi)|}-H^2\tau(\psi)\ln[r_{\rm m}(\psi)/C_4(\psi)]}\right|. \end{aligned} \tag{69}$$

This expression is only valid when the argument of logarithm is finite and not equal to zero for $r\in[r_{\rm m}(\psi),r_{\rm M}(\psi)]$.

We cannot have $\sigma(\psi)>0$ and $\tau(\psi)<0$ because in that case we would have $G^2<0$. Since ψ is expressed in terms of r and z by equation (39), equations (60)–(66) determine ρ as a function of r and z.

6.2 Wave damping

We start from transforming equation (34) to the variables r and ψ. We use the relation

$$\left.\frac{\partial h}{\partial\psi}\right|_\phi=\left.\frac{\partial h}{\partial\psi}\right|_r+\frac{\partial h}{\partial r}\frac{\partial r}{\partial\psi}, \tag{70}$$

where the subscripts ϕ and r indicate that the derivatives are taken at constant ϕ and constant r, respectively. Differentiating equation (54) and using equation (46) and the relation $J_0'(x)=-J_1(x)$ yields

$$\frac{\partial r}{\partial\psi}=\frac{HJ_0(r/H)J_1(r/H)}{\psi\left[J_0^2(r/H)+J_1^2(r/H)\right]}. \tag{71}$$

Now, using equations (18), (55) and (71), we transform equation (34) to

$$\frac{\partial Q}{\partial r}=-\Gamma(r,\psi)Q, \tag{72}$$

where

$$\begin{aligned} \Gamma(r,\psi)=&\frac{\omega\nu\lambda\left[J_0^2(r/H)+J_1^2(r/H)\right]}{2V_0^3rG^2\psi}\\ &\times\left(\frac{\psi}{J_1(r/H)}\frac{\partial h}{\partial\psi}+\frac{HJ_0(r/H)}{J_0^2(r/H)+J_1^2(r/H)}\frac{\partial h}{\partial r}\right)^2, \end{aligned} \tag{73}$$

and $\partial h/\partial\psi$ is calculated at constant r.

To characterize the efficiency of the wave damping, we calculate the variation with the height of the wave energy flux averaged over the wave period, Π, through surfaces $\phi=$ const. A surface $\phi=$ const is uniquely defined by the coordinate of the point of its intersection with the z-axis. Hence, Π is a function of z. Multiplying equation (2) by v, equation (3) by b/μ_0 and adding the results, we obtain

$$\begin{aligned} \frac{\partial}{\partial t}\left(\frac{\rho v^2}{2}+\frac{b^2}{2\mu_0}\right)=&\frac{1}{\mu_0}\nabla\cdot(\boldsymbol{B}vb)\\ &+\frac{v}{r}\frac{\partial}{\partial r}\left(\rho\nu r\frac{\partial v}{\partial r}\right)+v\frac{\partial}{\partial z}\left(\rho\nu\frac{\partial v}{\partial z}\right). \end{aligned} \tag{74}$$

The expression in the parentheses on the left-hand side of this equation is the wave energy density, while $-\boldsymbol{B}vb/\mu_0$ is the density of the wave energy flux. We obtain exactly the same expression for the density of the wave energy flux if we calculate the Pointing flux and only keep the quadratic terms. When $\nu=0$, equation (74) is the

energy conservation equation. If we take the average of equation (74) over the wave period, then we obtain that the average density of the wave energy flux is conserved as it should be. The density of the energy flux is directed along the equilibrium magnetic field. Equations (35) and (36) give the complex expressions for u and b. To obtain the physical quantities, we need to take the real parts of these expressions. Then, using equations (35) and (36), we obtain that the magnitude of the average over the period density of the wave energy flux is

$$-\frac{B}{\mu_0}\langle vb\rangle = \rho_0 V_0 H^2 Q^2 A_0^2 \frac{\lambda B}{2\omega B_0}, \tag{75}$$

where the angle brackets indicate the averaging over the period. Let Σ be the surface defined by the condition $\phi = -H\mathrm{e}^{-z_0/H}$. This surface crosses the z-axis at $z = z_0$. It follows from equations (38) and (42) that the equation of Σ is

$$\psi = \mathrm{e}^{-z_0/H}\frac{r J_1(r/H)}{J_0(r/H)}. \tag{76}$$

Using equation (39), we obtain that in cylindrical coordinates the equation of Σ is

$$z = z_0 + H\ln[J_0(r/H)]. \tag{77}$$

The wave energy flux through Σ is equal to the wave energy flux density integrated over the part of Σ that is inside the magnetic tube bounded by the surface $\psi = \psi_\mathrm{b}$. The elementary part of Σ is

$$d\Sigma = \sqrt{1+\left(\frac{\partial z}{\partial r}\right)^2}\, r\,\mathrm{d}r\,\mathrm{d}\theta = \sqrt{1+\frac{J_1^2(r/H)}{J_0^2(r/H)}}\, r\,\mathrm{d}r\,\mathrm{d}\theta. \tag{78}$$

Using equations (41) and (42) yields

$$\frac{B^2}{B_0^2} = \frac{\psi^2}{r^2}\left(1+\frac{J_0^2(r/H)}{J_1^2(r/H)}\right). \tag{79}$$

With the aid of this result and equation (71), we obtain from equations (78) $(B/B_0)\mathrm{d}\Sigma = H\,\mathrm{d}\psi\,\mathrm{d}\theta$. Then, taking into account that the energy flux at Σ is everywhere in the direction normal to this surface, we obtain with the aid of equation (75) that the average energy flux through the surface Σ is

$$\Pi(z) = -\frac{1}{\mu_0}\int_\Sigma B\langle vb\rangle\,\mathrm{d}\Sigma = \frac{\pi\rho_0 V_0 H^3}{\omega} \times \int_0^{\psi_\mathrm{b}}\sqrt{\omega^2+\sigma(\psi)}A_0^2(\psi)Q^2(r(\psi,z),\psi)\,\mathrm{d}\psi, \tag{80}$$

where $r(\psi, z)$ is defined by equation (76), and we dropped the subscript 0 at z because z_0 is an arbitrary point from the interval $(0, H\ln|H/\phi_2|)$. When $\nu = 0$, it follows from equation (72) that Q is independent of r, which implies that Π is independent of z, as it should be. The account of viscosity causes the decrease of Π with the height.

6.3 Particular case: $\sigma(\psi) > 0$ and $\tau(\psi) > 0$

6.3.1 Analytical investigation

We now consider the case where $\sigma(\psi) > 0$ and $\tau(\psi) > 0$, so G, ρ and h are defined by equations (66) and (68). We recall that r monotonically increases from $r_\mathrm{m}(\psi) \approx \sqrt{2H\psi}$ to $r_\mathrm{M}(\psi)$ with the distance along a particular magnetic field line (ψ = const). We take $C_4(\psi) \geq r_\mathrm{M}(\psi)$, so that $\ln[r/C_4(\psi)] \leq 0$ in equation (66) in the whole domain of variation of r and ψ shown in Fig. 3. We also impose a viable condition that ρ monotonically decreases along any magnetic field lines, which implies that it must be a monotonically decreasing function of r at fixed ψ. It is straightforward to obtain that this condition reduces to

$$\left(\ln\frac{r}{C_4(\psi)}\right)^2 + \ln\frac{r}{C_4(\psi)} + \frac{\psi^2 V_0^2\sigma(\psi)}{H^4\tau^2(\psi)} \geq 0. \tag{81}$$

We impose the condition

$$\sigma(\psi) \geq \frac{H^4\tau^2(\psi)}{4\psi^2 V_0^2}, \tag{82}$$

which guarantees that the inequality (81) is satisfied for any value of r. Now we put

$$C_4(\psi) = \kappa r_\mathrm{M}(\psi), \quad \sigma(\psi) = \frac{\chi^2 H^4\tau^2(\psi)}{\psi^2 V_0^2}, \tag{83}$$

where κ and χ are constants satisfying $\kappa \geq 1$ and $\chi \geq \frac{1}{2}$. Then equations (66) and (68) reduce to

$$\begin{aligned} G^2 &= \frac{H^4\tau(\psi)}{\psi^2 V_0^2}\left[\chi^2 + W^2(r,\psi)\right], \\ \rho &= \frac{\rho_0\psi^4 V_0^4}{r^4 H^4\tau^2(\psi)\left[\chi^2+W^2(r,\psi)\right]^2}, \\ h &= \frac{\psi V_0^2}{\chi H^2\tau(\psi)}\left[\arctan\frac{W_\mathrm{m}(\psi)}{\chi} - \arctan\frac{W(r,\psi)}{\chi}\right], \end{aligned} \tag{84}$$

where

$$W(r,\psi) = -\ln\frac{r}{\kappa r_\mathrm{M}(\psi)}, \quad W_\mathrm{m}(\psi) = -\ln\frac{r_\mathrm{m}(\psi)}{\kappa r_\mathrm{M}(\psi)}. \tag{85}$$

Equation (67) reduces to

$$\frac{\tau(\psi)}{\psi}\left[\chi^2 + \frac{1}{4}\left(\ln\frac{|\phi_2|}{\kappa^2 H}\right)^2\right] \to \frac{V_0^2}{2H^3} \quad \text{as} \quad \psi \to 0. \tag{86}$$

It is expedient to evaluate the variation of the Alfvén speed along the symmetry axis. It follows from equation (40) that at the symmetry axis $B = B_0\mathrm{e}^{-z/H}$. Using equations (39) and (50) yields $r = \sqrt{2H\psi}\,\mathrm{e}^{z/2H}$ and $r_\mathrm{M} = H\sqrt{-2\psi/\phi_2}$ when $\psi \ll |\phi_2|$. With the aid of these results, we obtain

$$W = \frac{1}{2}\ln\frac{\kappa^2 H}{|\phi_2|} - \frac{z}{2H}. \tag{87}$$

Then, using this equation and equation (86), we finally arrive at

$$\begin{aligned} \frac{\rho}{\rho_0} &= \left(\frac{4\chi^2+[\ln(\kappa^2 H/|\phi_2|)]^2}{4\chi^2+[\ln(\kappa^2 H/|\phi_2|)-z/H]^2}\right)^2 \mathrm{e}^{-2z/H} \\ \frac{V_\mathrm{A}}{V_0} &= \frac{4\chi^2+[\ln(\kappa^2 H/|\phi_2|)-z/H]^2}{4\chi^2+[\ln(\kappa^2 H/|\phi_2|)]^2}. \end{aligned} \tag{88}$$

It follows from equation (38) that the maximum value of z on the symmetry axis is $H\ln|H/\phi_2|$. Then the minimum value of the Alfvén speed at the symmetry axis, V_Am, is given by

$$\frac{V_\mathrm{Am}}{V_0} = \frac{4(\chi^2+\ln^2\kappa)}{4\chi^2+[\ln(\kappa^2 H/|\phi_2|)]^2}. \tag{89}$$

Since the expression for Φ_0 in equation (26) contains an arbitrary function $A(\psi)$, we can choose the dependence of Φ_0 on ψ arbitrarily. We take $\Phi_0 = \mathrm{e}^{-\mathrm{i}\omega t}$. Then it follows from equation (28) that $Q = 1$ at $h = 0$. The condition $h = 0$ is equivalent to $r = r_\mathrm{m}(\psi) \approx \sqrt{2H\psi}$. Hence, Q is defined by the solution to equation (72) satisfying the boundary condition

$$Q = 1 \quad \text{at} \quad r = \sqrt{2H\psi}. \tag{90}$$

To calculate $\Pi(z)$, we also need to define the function $A_0(\psi)$. To do this, we impose the boundary condition

$$u = u_0 \left(1 - \frac{r^2}{R_0^2}\right) \mathrm{e}^{-\mathrm{i}\omega t} \quad \text{at} \quad z = 0 \tag{91}$$

(we recall that R_0 is the tube radius at $z = 0$). It follows from equation (39) that the condition $z = 0$ is equivalent to $\psi = rJ_1(r/H)$, or $r \approx \sqrt{2H\psi} \approx r_\mathrm{m}(\psi)$. Then it follows from equations (84) and (85) that at $z = 0$

$$\rho \approx \rho_1(\psi) \equiv \frac{\rho_0 \psi^2 V_0^4}{4H^6\tau^2(\psi)} \left[\chi^2 + \left(\ln \frac{r_\mathrm{m}(\psi)}{\kappa r_\mathrm{M}(\psi)}\right)^2\right]^{-2}, \; h \approx 0. \tag{92}$$

Now it follows from equation (35) that

$$u = \frac{H A_0(\psi)}{\sqrt{2H\psi}} \left(\frac{\rho_0}{\rho_1(\psi)}\right)^{1/4} \mathrm{e}^{-\mathrm{i}\omega t} \quad \text{at} \quad z = 0. \tag{93}$$

Comparing equations (91) and (93) and using the relation $r^2 \approx 2H\psi$ yields

$$A_0(\psi) = \frac{u_0 \psi V_0}{H^2 \sqrt{\tau(\psi)\left[\chi^2 + W_\mathrm{m}^2(\psi)\right]}} \left(1 - \frac{2H\psi}{R_0^2}\right). \tag{94}$$

Using this result, we reduce equation (80) to

$$\Pi(z) = \frac{\pi \rho_0 u_0^2 V_0^2}{H} \int_0^{\psi_\mathrm{b}} Q^2(r(\psi, z), \psi) \left(1 - \frac{2H\psi}{R_0^2}\right)^2 \times \sqrt{\frac{1}{\tau^2(\psi)} + \frac{\chi^2 H^4}{\omega^2 \psi^2 V_0^2}} \frac{\psi^2 \, \mathrm{d}\psi}{\chi^2 + W_\mathrm{m}^2(\psi)}. \tag{95}$$

We also need the expression for Γ. Differentiating the second identity in equation (50), and using equation (47) and the identity $J_0'(x) = -J_1(x)$ yields

$$\frac{\mathrm{d}r_\mathrm{M}}{\mathrm{d}\psi} = -\frac{H^2 Y(\psi)}{r_\mathrm{M}\phi_2}, \quad Y(\psi) = \frac{J_0^2(r_\mathrm{M}/H)}{J_0^2(r_\mathrm{M}/H) + J_1^2(r_\mathrm{M}/H)}. \tag{96}$$

Differentiating the expression for h given by equation (84) with respect to r, we obtain

$$\frac{\partial h}{\partial r} = \frac{\psi V_0^2}{r H^2 \tau(\psi)\left[\chi^2 + W^2(r, \psi)\right]}. \tag{97}$$

Differentiating the expression for h with respect to ψ yields

$$\frac{\partial h}{\partial \psi} = \frac{V_0^2}{\chi H^2 \tau(\psi)} \left[\arctan \frac{W_\mathrm{m}(\psi)}{\chi} - \arctan \frac{W(r, \psi)}{\chi}\right] \times \left(1 - \frac{\psi}{\tau(\psi)} \frac{\mathrm{d}\tau}{\mathrm{d}\psi}\right) + \frac{\psi V_0^2 Y(\psi)}{\phi_2 2\tau(\psi) r_\mathrm{M}^2(\psi)\left[\chi^2 + W^2(r, \psi)\right]} - \frac{V_0^2}{H^2 \tau(\psi)\left[\chi^2 + W_\mathrm{m}^2(\psi)\right]} \left(\frac{\psi H^2 Y(\psi)}{\phi_2 r_\mathrm{M}^2(\psi)} + \frac{1}{2}\right). \tag{98}$$

Then Γ is defined by equations (73), (84) and (96)–(98).

6.3.2 Numerical results

The dependence of the wave energy flux Π on z was calculated numerically. Below we take the density at the tube base given by

$$\rho = \frac{\rho_0}{\zeta} \begin{cases} 1 + (\zeta - 1)\left(1 - \dfrac{r^2}{R_0^2}\right)^2, & r \le R_0, \\ 1, & r \ge R_0, \end{cases} \tag{99}$$

where ζ is the ratio of the density at the tube axis to the density outside the tube. Using equation (39), we obtain the approximate expression

$$r = \sqrt{2H\psi} \, \mathrm{e}^{z/2H} \tag{100}$$

valid for $r \ll H$. Since $\psi \le \psi_\mathrm{b} \ll H$, this condition is satisfied for $r \le R_0$. In particular, at the tube base $r = \sqrt{2H\psi}$. Then we can rewrite equation (99) as

$$\frac{\rho}{\rho_0} = q(\psi) \equiv \frac{1}{\zeta} \begin{cases} 1 + (\zeta - 1)\left(1 - \dfrac{\psi}{\psi_\mathrm{b}}\right)^2, & r \le \psi_\mathrm{b}, \\ 1, & r \ge \psi_\mathrm{b}. \end{cases} \tag{101}$$

On the other hand, it follows from equation (84) that at the tube base

$$\rho = \frac{\rho_0 \psi^2 V_0^4}{4H^6 \tau^2(\psi)\left[\chi^2 + W_\mathrm{m}^2(\psi)\right]^2}, \quad \psi \le \psi_\mathrm{b}. \tag{102}$$

The expression for ρ beyond the tube boundary is obtained by substituting ψ_b for ψ in this expression. Comparing equations (101) and (102), we obtain that the expression for $\tau(\psi)$ valid for $\psi \le \psi_\mathrm{b}$ is given by

$$\tau(\psi) = \frac{\psi V_0^2 \sqrt{\zeta}}{2H^3[\chi^2 + W_\mathrm{m}^2(\psi)]} \left[1 + (\zeta - 1)\left(1 - \frac{\psi}{\psi_\mathrm{b}}\right)^2\right]^{-1/2}. \tag{103}$$

It is straightforward to see that this expression agrees with equation (86).

It is a very popular assumption that the corona is isothermal. In that case, the plasma density is given by

$$\rho = \rho_0 \mathrm{e}^{-z/H_\rho}, \tag{104}$$

where H_ρ is the density scaleheight. Unfortunately, the equilibria with an isothermal plasma and exponentially divergent magnetic field lines are not non-reflective. We try to approximate the density given by equation (104) by that given by equation (88) at the tube axis. We take the maximum height at the symmetry axis equal to $6H$. Since this maximum height is $H\ln|H/\phi_2|$, this implies that $\ln|H/\phi_2| = 6$. Then the expression for the density at the tube axis given by equation (88) reduces to

$$\frac{\rho}{\rho_0} = \left(\frac{\chi^2 + (\varsigma + 3)^2}{\chi^2 + (\varsigma + 3 - z/2H)^2}\right)^2 \mathrm{e}^{-2z/H}, \tag{105}$$

where $\varsigma = \ln\kappa$. First condition that we impose is that the values of ρ given by equations (104) and (105) coincide at $z = 6H$. This results in the equation

$$\frac{\chi^2 + (\varsigma + 3)^2}{\chi^2 + \varsigma^2} = \exp\left[3\left(2 - \frac{H}{H_\rho}\right)\right] \equiv E. \tag{106}$$

This is the equation determining χ as a function of ς. Since the left-hand side of this equation is larger than unity, a necessary condition that it has a solution is $H_\rho \ge H/2$, $H_\rho = H/2$ corresponding to $\chi \to \infty$. It follows from equation (106) that

$$\chi^2 = \frac{(\varsigma + 3)^2 - E\varsigma^2}{E - 1}. \tag{107}$$

Substituting this result in equation (105) yields

$$\frac{\rho}{\rho_0} = \frac{9E^2(2\varsigma + 3)^2 \mathrm{e}^{-2z/H}}{\{[3E - (E - 1)z/2H](2\varsigma + 3 - z/2H) + 3z/2H\}^2}. \tag{108}$$

The condition $\chi \ge 1/2$ imposes a restriction on ς,

$$4(E - 1)\varsigma^2 - 24\varsigma + E - 37 \le 0. \tag{109}$$

This inequality only can be satisfied if the discriminant of the left-hand side considered as a quadratic polynomial of ς is non-negative. This condition is written as

$$E^2 - 38E + 1 \leq 0. \tag{110}$$

This condition is equivalent to $E \leq 19 + 6\sqrt{10} \approx 37.97$, which, in turn, implies that

$$H_\rho \leq \frac{3H}{6 - \ln(19 + 6\sqrt{10})} \approx 1.27H.$$

Hence, eventually we obtain that H_ρ must satisfy

$$0.5H \leq H_\rho \leq 1.27H. \tag{111}$$

Then it follows from equation (109) that

$$\max\left(0, \frac{6 - S}{2(E-1)}\right) \leq \varsigma \leq \frac{6 + S}{2(E-1)}, \tag{112}$$

where

$$S = \sqrt{38E - E^2 - 1}, \tag{113}$$

and we took into account that $\varsigma \geq 0$. We note that $\frac{1}{2}(6 - S)/(E - 1) \leq 0$ when $0.83H \leq H_\rho \leq 1.14H$, while $\frac{1}{2}(6 - S)/(E - 1) > 0$ otherwise.

In the expression for ρ given by equation (108), we still have one free parameter ς. We choose this parameter to make the density dependence on z given by equation (108) as close to that given by equation (104) as possible. The mean square deviation of the densities given by equations (104) and (108) is proportional to the square root of the following integral:

$$I(\varsigma) = 2H \times \int_0^3 \left(\mathrm{e}^{-2zH/H_\rho} - \frac{9E^2(2\varsigma + 3)^2\mathrm{e}^{-4z}}{\{[3E - (E-1)z](2\varsigma + 3 - z) + 3z\}^2}\right)^2 \mathrm{d}z. \tag{114}$$

To derive this expression, we used equation (107), made the substitution $z' = z/2H$ and then dropped the prime. We choose the value of ς that minimizes $I(\varsigma)$.

In Fig. 4, the two dependences of ρ on z, one given by equation (104) and the other by equation (108), are shown for various values of H_ρ/H. We see that the accuracy of the approximation of the exponentially decreasing density profile by the density profile defined by equation (108) increases when H_ρ/H decreases. Note that the two expressions coincide for $H_\rho/H = \frac{1}{2}$.

We calculated the dependence of $\Delta = \Pi(z)/\Pi(0)$ on z/H. This function depends on four dimensionless parameter: R_0/H, H_ρ/H, $\omega H/V_0$ and the Reynolds number $\mathrm{Re} = HV_0/\nu$. In all our calculations, we took $R_0/H = 0.1$ and $H_\rho/H = 1.25$, which is slightly below the maximum possible value $H_\rho/H = 1.27$. Keeping in mind the application to coronal plumes, we take the electron number density at the centre of the plume equal to $10^{15}\,\mathrm{m}^{-3}$. We also take the density contrast between the plume centre and far from $\zeta = 5$. If we also take $B = 10\,\mathrm{G}$, then we obtain for the Alfvén it equal to speed in the plume centre $V_0 \approx 700\,\mathrm{km\,s}^{-1}$. Taking H varying from 30 to 60 Mm and the wave period varying from 30 to 60 s, we obtain that the minimum and maximum values of $\omega H/V_0$ are $10\pi/7$ and $40\pi/7$, respectively.

If we take the plasma temperature equal to 10^6 K, then the classical plasma theory gives for the ion collisional time $\tau_i = 1$ s and $10^{10}\,\mathrm{m}^2\,\mathrm{s}^{-1}$ for the first coefficient in the expression for the full Braginskii viscosity tensor (Spitzer 1962; Braginskii 1965). However, the presence of magnetic field makes the viscosity in the solar corona strongly anisotropic. The first term in the Braginskii expression for the viscosity tensor describes the volume viscosity that does not affect Alfvén waves. The Alfvén wave damping is caused by shear viscosity. The shear viscosity is smaller than the volume viscosity by factor $(\tau_i\omega_i)^{-2}$, where ω_i is the ion gyrofrequency. For $B = 10\,\mathrm{G}$, we obtain $\omega_i \approx 10^5\,\mathrm{s}^{-1}$. As a result, we obtain $\nu \approx 1\,\mathrm{m}^2\,\mathrm{s}^{-1}$. But this estimate must be taken with caution. It is quite possible that turbulence can greatly enhance shear viscosity. Therefore, it seems reasonable to consider ν as a free parameter. We considered four values of ν, 10^5, 10^6, 3×10^6 and $10^7\,\mathrm{m}^2\,\mathrm{s}^{-1}$. The corresponding values of Re are 2.1×10^7, 2.1×10^6, 7×10^6 and 2.1×10^6 when $H = 30$ Mm, and 4.2×10^7, 4.2×10^6, 1.4×10^7 and 4.2×10^6 when $H = 60$ Mm. The dependence of Δ on z is shown in Fig. 5.

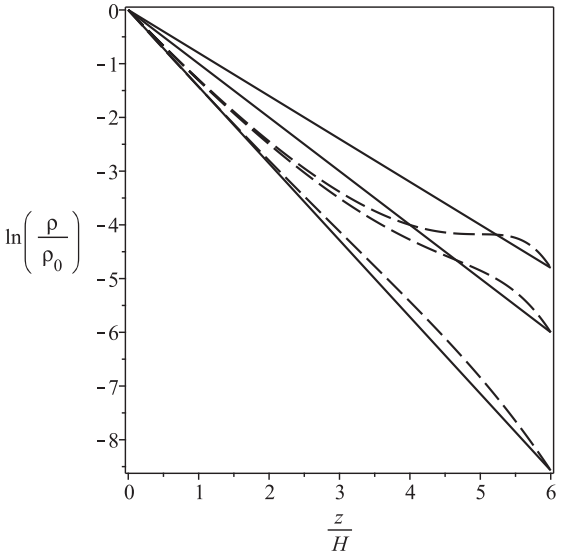

Figure 4. Dependence of density ρ on z at the tube axis ($r = 0$). The solid curves show the dependence defined by equation (104), and the dashed by equation (108). The top, middle and bottom curves correspond to $H_\rho/H = 1.25$, 1 and 0.7.

First of all, Fig. 5 reveals that the damping rate strongly depends on the value of ν, which, of course, is an expected result. The solid curves showing the dependence of Δ on z/H are almost horizontal, which implies that the damping is practically negligible when $\nu = 10^5\,\mathrm{m}^2\,\mathrm{s}^{-1}$. The wave damping is only substantial when $\nu = 10^7\,\mathrm{m}^2\,\mathrm{s}^{-1}$, which is by seven orders of magnitude larger than the value given by the classical plasma theory. Comparing the upper and lower panels in Fig. 5, we see that the damping of waves with the period of 30 s is much stronger than that of waves with the period of 60 s, which is again an expected result. Finally, comparing the left- and right-hand panels in Fig. 5 shows that the reduction in the wave energy flux at the height $6H$ is slightly higher for $H = 60$ Mm than for $H = 30$ Mm. However, we must keep in mind that $6H = 180$ Mm when $H = 30$ Mm, while $6H = 360$ Mm when $H = 60$ Mm.

It is expedient to compare these results with the damping of phase-mixed Alfvén waves in a magnetic plasma configuration with the straight magnetic field lines. We consider an axisymmetric equilibrium with constant magnetic field and the density approximating the exponential decay. The dependence of the wave density flux on height is calculated in Appendix A. Using equation (A15), we calculated the ratio of the density flux at $z = 6H$ and $z = 0$, $\Delta(6H)$, for a few values of H and the wave period T. In this calculation, we took $V_0 = 700\,\mathrm{m\,s}^{-1}$, $\nu = 10^7\,\mathrm{m}^2\,\mathrm{s}^{-1}$ and $H_\rho/H = 1.25$. The

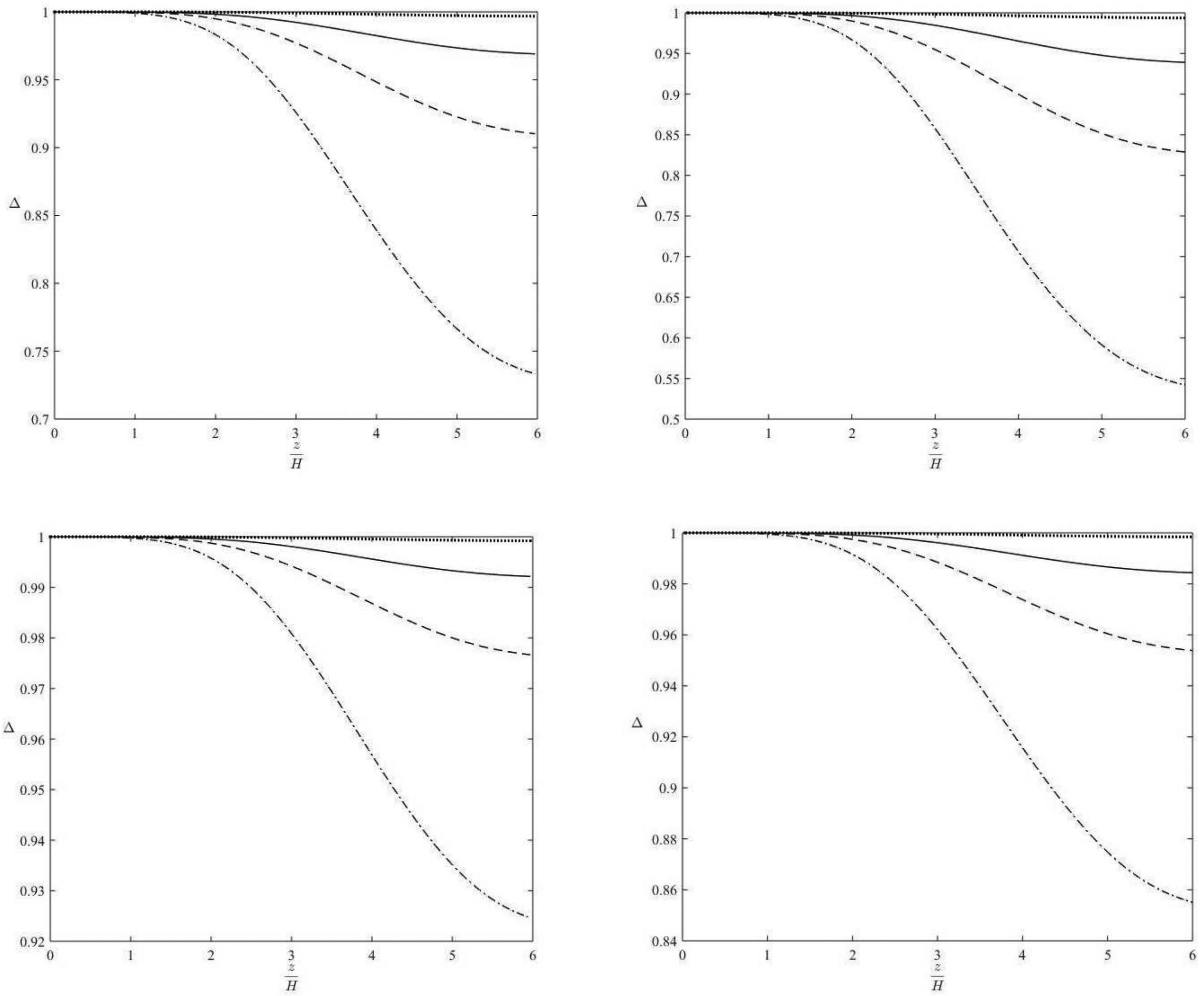

Figure 5. Dependence of Δ on z for $H_\rho/H = 1.25$. The left-hand panels correspond to $H = 30$ Mm, and the right to $H = 60$ Mm. The upper panels correspond to the wave period equal to 30 s, and the lower to the wave period equal to 60 s. The solid, dashed, dotted and dash–dotted curves correspond to $\nu = 10^5, 10^6, 3 \times 10^6$ and 10^7 m^2 s^{-1}, respectively.

Table 1. Results.

	$H = 30$ Mm	$H = 60$ Mm
$T = 30$ s	0.993	0.987
$T = 60$ s	0.998	0.996

results are given in Table 1. We see that the wave damping at the height $6H$ in the equilibrium with the straight magnetic field lines is practically negligible. This result clearly shows that the exponential divergence of the magnetic field lines results in the enhanced damping of phase-mixed Alfvén waves.

We also studied the dependence of Δ calculated at $z = 6H$ on H_ρ/H. In this study, we took $\nu = 10^7$ m^2 s^{-1}. The results are shown in Fig. 6. As we have already seen, H_ρ/H can vary from 0.5 to 1.27. However, we slightly reduced the upper boundary and considered $0.5 \leq H_\rho/H \leq 1.25$. We see that the efficiency of wave damping quickly increases with the increase of H_ρ/H. This result enables us to clarify the physical reason of the enhanced wave damping in equilibria with exponentially divergent magnetic field lines. In such an equilibrium, the magnetic field magnitude decreases as $e^{-z/H}$. Then the Alfvén speed decreases as $\exp[-z/(H - H_\rho/2)]$. Since the wave frequency is fixed, the decrease in the Alfvén speed

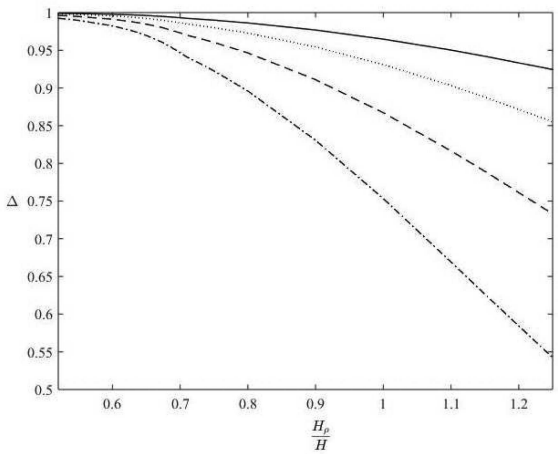

Figure 6. Dependence of Δ calculated at $z = 6H$ on H_ρ/H. This dependence is calculated for $\nu = 10^7$ m^2 s^{-1}. The solid curve corresponds to $H = 30$ Mm and the wave period 60 s, the dotted curve to $H = 60$ Mm and the wave period 60 s, the dashed curve to $H = 30$ Mm and the wave period 30 s, and the dash–dotted curve to $H = 60$ Mm and the wave period 30 s.

causes the decrease in the wavelength and increases the time needed for the wave to reach a definite height. This increases the efficiency of the wave damping. The larger H_ρ/H, the stronger the decrease in the Alfvén speed is, and then the more efficient the wave damping is. Now it is clear why the wave damping obtained in this paper is slightly less efficient than that obtained by Ruderman & Petrukhin (2017). The reason is that Ruderman & Petrukhin (2017) considered an equilibrium with the constant density, while here we considered the density decaying with the height.

7 SUMMARY AND CONCLUSIONS

In this paper, we studied the damping of phase-mixed Alfvén waves in axisymmetric non-reflective magnetic plasma configurations. We derived the general expression describing the damping of phase-mixed Alfvén waves when they propagate along the magnetic field lines. Then we applied the general theory to a particular case of equilibrium with exponentially divergent magnetic field lines. The condition that the equilibrium is non-reflective determines the density dependence on spatial coordinates. Exponentially decreasing with the height density is, in general, not among the set of density profiles determined by the non-reflective condition. However, we obtained the density profiles that fairly well approximate the exponentially decaying density. We calculated the dependence on the height of the total average over the period wave density flux propagating in a magnetic tube. We considered waves with the periods of 30 and 60 s, and the magnetic scaleheight H equal to 30 and 60 Mm. We obtained that a substantial wave damping at the height $6H$ is only possible if the shear viscosity ν is enhanced by seven orders of magnitude in comparison with the value given by the classical plasma theory and taken to be $\nu = 10^7\,\mathrm{m^2\,s^{-1}}$. With this value of shear viscosity, depending on the wave period and H, from 7 per cent to 45 per cent of the wave energy is dissipated until the wave reaches the height $6H$.

As we can expect, the dissipation efficiency strongly depends on the wave period. When $H = 30$ Mm, 27 per cent of the wave energy dissipates when the wave period is 30 s, while only 7 per cent of the wave energy dissipates when the wave period is 60 s. For $H = 60$ Mm, these numbers are 45 per cent and 14.5 per cent, respectively. An important result that we obtained is that the wave damping in magnetic plasma configurations with exponentially divergent magnetic field lines strongly depends on the density variation with the height. The stronger the density decrease, the weaker the wave damping is. This result enabled us to give the physical explanation of the phenomenon of the enhanced wave damping caused by the exponential divergence of the magnetic field lines. Due to this divergence, the magnetic field magnitude exponentially decreases with the height. If the density does not change with the height or decreases slower than the magnetic field magnitude, then the Alfvén speed exponentially decreases with the height. As a result, Alfvén waves propagating upwards have more time for damping than in the case when they propagate in an equilibrium with the constant or increasing with the height Alfvén speed.

Of course, it is difficult to expect that the real magnetic plasma configurations in the solar atmosphere are non-reflective. However, we hope that at least some of these configurations are close to non-reflective in the sense that the wave reflection in such configurations is very weak. The properties of wave propagation and damping in such configurations are very close to those in non-reflective configurations. In our future study, we will investigate what configurations with the exponentially expanding magnetic field lines and the density exponentially decreasing with the height are close to non-reflective.

ACKNOWLEDGEMENTS

The authors gratefully acknowledge financial support from the Russian Fund for Fundamental Research (RFFR) grant RFBR (16-02-00167). MSR acknowledges the support from the STFC grant.

REFERENCES

Abramowitz M., Stegun I. A., 1964, Handbook of Mathematical Functions with Formulas, Graphs, and Mathematical Tables, 10th edn. Dover Press, New York
Arregui I., 2015, Phil. Trans. R. Soc. A, 373, 20140261
Bender C. M., Orszag S. A., 1999, Advanced Mathematical Methods for Scientists and Engineers. Springer-Verlag, Berlin
Botha G. J. J., Arber T. D., Nakariakov V. M., Keenan F. P., 2000, A&A, 368, 1186
Braginskii S. J., 1965, in Leontovich M. A., ed., Reviews of Plasma Physics, Vol. 1, Consultants Bureau, New York, p. 205
Brekhovskikh L. M., 1980, Waves in Layered Media. Academic Press, New York
Didenkulova I., Pelinovsky E., Soomere T., 2008, Est. J. Eng., 14, 220
Ginzburg V. L., 1970, Propagation of Electromagnetic Waves in Plasma. Pergamon Press, Oxford
Grimshaw R., Pelinovsky E., Talipova T., 2010, J. Phys. Oceanogr., 40, 802
Heyvaerts J., Priest E. R., 1983, A&A, 117, 220
Ibragimov N. H., Rudenko O. V., 2004, Acta Phys., 50, 406
Malara F., Primavera L., Veltri P., 1996, ApJ, 459, 347
Nakariakov V. M., Roberts B., Murawski K., 1997, Sol. Phys., 175, 93
Petrukhin N. S., Pelinovsky E. N., Batsyna E. K., 2011, JETP Lett., 93, 564
Petrukhin N. S., Pelinovsky E. N., Batsyna E. K., 2012, Astron. Lett., 38, 388
Petrukhin N. S., Ruderman M. S., Pelinovsky E. N., 2015, Sol. Phys., 290, 1323
Ruderman M. S., Petrukhin N. S., 2017, A&A, 600, A122
Ruderman M. S., Nakariakov V. M., Roberts B., 1998, A&A, 338, 1118
Ruderman M. S., Petrukhin N. S., Pelinovsky E., Talipova T., 2013, Sol. Phys., 286, 417
Smith P. G., Tsiklauri D., Ruderman M. S., 2007, A&A, 475, 1111
Soler R., Terradas J., Oliver R., Ballester J. L., 2017, ApJ, 840, 20
Spitzer R., 1962, Physics of Fully Ionized Gases. Interscience, New York
Tsiklauri D., Nakariakov V. M., 2002, A&A, 393, 321
Tsiklauri D., Arber T. D., Nakariakov V. M., 2001, A&A, 379, 1098
Tsiklauri D., Arber T. D., Nakariakov V. M., 2002, A&A, 395, 285
Tsiklauri D., Nakariakov V. M., Rowlands G., 2003, A&A, 400, 1051
Tsuneta S. et al., 2008, ApJ, 688, 1374

APPENDIX A: DAMPING OF PHASE-MIXED ALFVÉN WAVES IN EQUILIBRIUM WITH STRAIGHT MAGNETIC FIELD LINES

We consider the axisymmetric equilibrium with the straight magnetic field lines. The magnetic field magnitude is constant and equal to B_0. In this case, it follows from equation (1) that

$$\phi = z, \quad \psi = \frac{r^2}{2H}. \tag{A1}$$

Hence, in what follows, we write z instead of ϕ. Equation (20) reduces to

$$X^3 \frac{\partial^2 X}{\partial z^2} = \frac{\sigma(\psi)}{V_0^2}, \tag{A2}$$

where $X = (\rho_0/\rho)^{1/4}$. We look for the solution to this equation in the from

$$X = \tilde{\sigma}^{1/4}(\psi)\sqrt{a_1(z/H)^2 + a_2}, \tag{A3}$$

where $\tilde{\sigma}(\psi) = V_0^2\sigma(\psi)/H^2$, and a_1 and a_2 are the quantities to be determined. Substituting this expression in equation (A2), we obtain that X satisfies equation (A2) if these quantities are related by $a_1a_2 = 1$. Hence,

$$\rho = \frac{\rho_0}{\tilde{\sigma}(\psi)}\left[a_1\left(\frac{z}{H}\right)^2 + \frac{1}{a_1}\right]^{-2}, \tag{A4}$$

where a_1 is arbitrary constant. Now we assume that ρ at $z = 0$ is given by equation (101). As a result, we obtain

$$\tilde{\sigma}(\psi) = a_1^2 q^{-1}(\psi). \tag{A5}$$

In addition, we impose the condition that

$$\rho(\psi, 6H) = \rho_0 q(\psi)\exp(-6H/H_\rho). \tag{A6}$$

Then equations (A4) and (A5) reduce to

$$\rho = \frac{\rho_0 q(\psi)}{[(sz/6H)^2 + 1]^2}, \tag{A7}$$

$$\sigma(\psi) = \frac{s^2 V_0^2}{36H^2 q(\psi)}, \tag{A8}$$

where

$$s = \sqrt{\exp(3H/H_\rho) - 1}. \tag{A9}$$

In Fig. A1, the graphs of $\rho(z)$ and $V_\mathrm{A}(z)$ at $\psi = 0$ with the density determined by equations (104) and (A7) are shown.

We see that equation (A7) fairly well approximates the exponentially decreasing density. Substituting equation (A7) in equation (17) and taking $\phi_1 = 0$ yields

$$h = \frac{6H\sqrt{q(\psi)}}{s}\arctan\frac{sz}{6H}. \tag{A10}$$

Using this result, we obtain from equation (34)

$$\Upsilon = \frac{36\nu\omega\lambda H\psi(\zeta-1)^2(1-\psi/\psi_\mathrm{b})^2}{s^2\zeta^2\psi_\mathrm{b}^2 V_0^3\sqrt{q(\psi)}[s^2(z/6H)^2+1]}\left(\arctan\frac{sz}{6H}\right)^2. \tag{A11}$$

$Q(z)$ is defined by equation (34) with z substituted for ϕ, and the boundary condition $Q = 1$ at $z = 0$. The solution to this boundary value problem is

$$Q = \exp\left(-\frac{72\nu\omega\lambda H\psi(\zeta-1)^2}{s^2\zeta^2\psi_\mathrm{b}^2 V_0^3\sqrt{q(\psi)}}\left(1-\frac{\psi}{\psi_\mathrm{b}}\right)^2\left(\arctan\frac{sz}{6H}\right)^3\right). \tag{A12}$$

We assume that u is defined by equation (91) at $z = 0$. On the other hand, it follows from equations (35) and (A7) that

$$u = A_0(\psi)\left(\frac{H^2}{4\psi^2 q(\psi)}\right)^{1/4}\mathrm{e}^{-\mathrm{i}\omega t} \quad \text{at} \quad z = 0. \tag{A13}$$

Comparing equations (91) and (A13) and taking into account that $R_0^2 = 2H\psi_\mathrm{b}$, we obtain

$$A_0(\psi) = u_0\left(1-\frac{\psi}{\psi_\mathrm{b}}\right)\left(\frac{4\psi^2 q(\psi)}{H^2}\right)^{1/4}. \tag{A14}$$

The magnitude of the average over the period density of the wave energy flux is given by equation (75) with B_0 substituted for B. The total energy flux through the surface $z = \mathrm{const}$ is equal to the integral of this flux over the circle of radius $R_0 = \sqrt{2H\psi_\mathrm{b}}$. It reads

$$\Pi(z) = \frac{2\pi\rho_0 u_0^2 V_0 H^2}{\omega}\int_0^{\psi_\mathrm{b}} Q^2\psi\lambda\sqrt{q(\psi)}\left(1-\frac{\psi}{\psi_\mathrm{b}}\right)^2\mathrm{d}\psi. \tag{A15}$$

Using this expression, we can calculate the relative energy flux $\Delta(z) = \Pi(z)/\Pi(0)$.

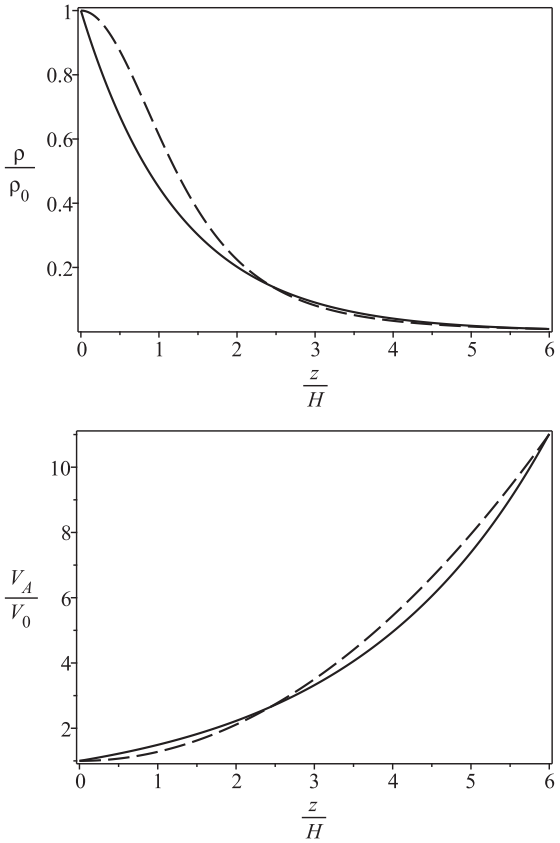

Figure A1. Dependence of ρ (upper panel) and V_A (lower panel) on z at $r = 0$ with the density defined by equation (104) (solid line) and by equation (A7) (dashed line) for $H_\rho/H = 1.25$.

This paper has been typeset from a TEX/LATEX file prepared by the author.